Finding and Navigating to Household Objects with UHF RFID Tags by Optimizing RF Signal Strength

Travis Deyle, Matthew S. Reynolds, and Charles C. Kemp

***Abstract*— We address the challenge of finding and navigating to an object with an attached ultra-high frequency radio-frequency identification (UHF RFID) tag. With current off-the-shelf technology, one can affix inexpensive self-adhesive UHF RFID tags to hundreds of objects, thereby enabling a robot to sense the RF signal strength it receives from each uniquely identified object. The received signal strength indicator (RSSI) associated with a tagged object varies widely and depends on many factors, including the object's pose, material properties and surroundings. This complexity creates challenges for methods that attempt to explicitly estimate the object's pose. We present an alternative approach that formulates finding and navigating to a tagged object as an optimization problem where the robot must find a pose of a directional antenna that maximizes the RSSI associated with the target tag. We then present three autonomous robot behaviors that together perform this optimization by combining global and local search. The first behavior uses sparse sampling of RSSI across the entire environment to move the robot to a location near the tag; the second samples RSSI over orientation to point the robot toward the tag; and the third samples RSSI from two antennas pointing in different directions to enable the robot to approach the tag. We justify our formulation using the radar equation and associated literature. We also demonstrate that it has good performance in practice via tests with a PR2 robot from Willow Garage in a house with a variety of tagged household objects.**

I. Introduction

Human environments contain a wide variety of objects, which often move within the environment and are hidden by other objects. This makes identification of objects and navigation to them using cameras and other line-of-sight sensors difficult for robots. One approach to overcoming these challenges is to affix ultra-high frequency (UHF) radio-frequency identification (RFID) tags to objects. Robots can then use each tag's unique identifier and the signal strength received from each tag (received signal strength indicator - RSSI) to identify and navigate to tagged objects.

UHF RFID tags have a number of desirable properties. The tags we use are small, thin, low-cost (e.g., sub-$0.10), self-adhesive, and fully passive (no battery). Using commercially-available UHF RFID readers, a robot can detect these tags from a distance (up to $3\,\mathrm{m}$ in practice) even when the line-of-sight between the reader antenna and the tag is occluded. Owing to anti-collision protocols between the reader and tags, hundreds of tags can coexist in the environment without interference. Furthermore, tag detections occur with effectively zero false positives, and the robot can either query for all tags at once or selectively query for a single tag out of all nearby tags [1].

In spite of these benefits, robot navigation to UHF RFID tagged objects in human environments presents significant challenges. In particular, the signal received from a tagged object by a robot's antenna varies drastically with changes in the object's pose, the object's materials, and the RF properties of the surrounding environment. Our goal is to enable robots to find and navigate to everyday objects in a human environment. As such, the pose of a tagged object and its surrounding environment can change in unexpected ways. In addition, we would like people to be able to affix tags to objects of their choosing without requiring expertise or extensive calibration.

Fig. 1. Two final robot configurations after performing our UHF RFID search algorithm for a tagged object on a fireplace mantle and inside a kitchen cabinet. Object locations are denoted by red circles.

The contributions of this paper are three-fold. First, we use insights from the radar equation to develop three robot behaviors for finding and navigating to UHF RFID tags. These behaviors do not require an explicit sensor model, nor do they require extensive data-driven training or calibration.

Second, we unify our behavior-based methods into a common mathematical optimization framework. We formulate finding and navigating to a tagged object as an optimization problem where the robot must find a pose of a directional antenna that maximizes the RSSI from a tag with an ID corresponding with the target object (the target tag).

Finally, we demonstrate that our approach can enable a PR2 from Willow Garage to find and navigate to a variety of tagged household objects within a real home. We show that the robot can efficiently perform this optimization with good results by combining global search based on sparse sampling, and local search akin to gradient ascent. We show that our behaviors result in a final robot position close to the target tag and an orientation pointed toward it – a generally useful capability.

II. Related Work

Robotics has been a motivating application for RFID since the dawn of modern RFID technologies in the 1990s [2]. Since then, roboticists have leveraged the capabilities of

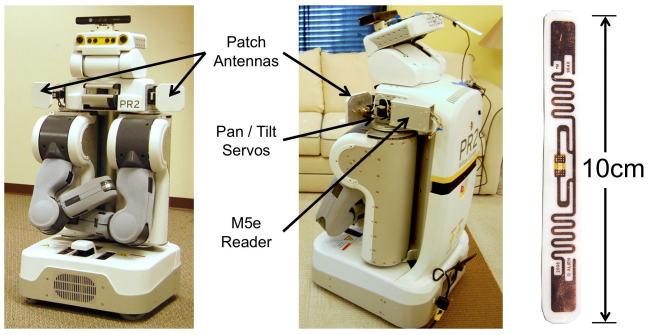

Fig. 2. **Left:** Our PR2 robot uses two actuated, shoulder-mounted UHF RFID antennas to search for tagged objects. **Right:** The Alien ALN-9640 Squiggle UHF RFID tag that we applied to most objects for this paper.

RFID to great effect. The unique identifier has proved useful for object recognition [3], as a high-confidence landmark in SLAM implementations [4], for waypoint navigation [5], and as a complementary sensing modality for multi-sensor fusion [6]. Many of these systems rely on low-frequency (LF) and high-frequency (HF) RFID tags. Their shorter read ranges (5-10 cm) provide a straight-forward tag position estimate, since a positive read indicates that the tag is nearby. However, short read range can have drawbacks, such as requiring many more tags or readers, and requiring a robot to search at a fine granularity to locate a tagged object. Ultra-high frequency (UHF) RFID tags offer a compelling alternative, since tags can be detected from a distance of several meters. However, UHF RFID readers do not provide precise tag location information.

The currently-dominant approach to finding and navigating to UHF RFID tags is to first explicitly estimate the tag's pose (relative to the robot or on a map) using Bayesian localization with a data-driven sensor model. The sensor models distinguish previous research efforts and include models based on: RF propagation [7], snapshots and fingerprinting [8], tag detection [9], and tag detection plus RSSI [10]. Researchers have demonstrated tag localization uncertainties between 30-70 cm when localizing tags attached to walls, floors, and other fixed locations in buildings. These results rely on the assumption of a relatively-uncluttered environment with substantial free space, and that the tag's orientation and nearby material properties have relatively-little variation from place to place. However, it is well-known within the RFID community that tagging objects causes RSSI signals to vary widely based on the object's 6-DoF pose [11], material properties [12], and multipath as the object is relocated to new, unmodeled environments [13]. Characterizing and modeling the impact of these factors on Bayesian tag localization is an unsolved challenge and remains a persistent area of research within the robotics, RFID, and radar communities.

In this paper, we present an alternative approach to finding and navigating to UHF RFID tagged objects that draws insights from the rich history of behavior-based robotic source localization, including: chemical plume tracing [14], gradient-following or gradient-field algorithms [15], and various forms of biologically-inspired taxis (e.g., chemotaxis or phototaxis) [16]. These methods do not explicitly estimate the pose of a source. Instead, the approximate source location is often estimated as the final position of a mobile robot after it has performed various behaviors that try to maximize sensor measurements related to the sought-after stimulus [17].

UHF RFID poses unique challenges compared to sound-source or odor-source localization. The source of interest is a backscattered (reflected) RF signal being generated by an RFID tag. RF signal measurements are governed by RF propagation effects such as multipath, shadowing, diffraction, tag and antenna pose, as well as environment and tagged-object material properties. Even in unobstructed free space, received signals can change from a maximum peak (constructive interference) to a minimum null (destructive interference, potentially resulting in no tag detection) in as little as one wavelength ($33\,\mathrm{cm}$), and low-level UHF RFID protocols deliberately introduce stochasticity to facilitate channel sharing in tag-dense environments [18].

Earlier work in the literature suggests that behavior-based methods may indeed be applicable to UHF RFID source localization. Much of this related work focuses on UHF RFID tags attached to walls, floors, and other fixed locations in buildings where tag orientation and nearby material properties are constrained. Examples include bearing estimation for robot localization [19], RFID servoing for autonomous robot docking [20], and path following [21]. This paper builds on this and our own prior work [22].

III. Finding and Navigating as Optimization

We formulate our approach as an optimization problem, where the robot searches for a 6-DoF pose, P^*, of a directional reader antenna that maximizes the expected value of the signal strength, $RSSI$, received from a tag with a target ID. We denote the general optimization problem as

$$P^* = \underset{P}{\operatorname{argmax}} \ \mathsf{E}\left(\boldsymbol{RSSI} \mid \boldsymbol{P} = P \right). \tag{1}$$

We represent RSSI values reported by the robot's reader antennas as being samples from a random variable, $RSSI$. Even with fixed pose, RSSI values vary due to a variety of factors, including noise and stochasticity intentionally introduced by communication protocols. For most of the methods in this paper, we estimate the expected value of $RSSI$ using the sample mean.

As we will justify in the following sections through an idealized model of RF propagation and real-world testing, performing this optimization results in an antenna pose that is both close to the target tag and oriented toward it. To simplify our presentation, throughout most of this paper we will assume that the reader antenna achieving a pose implies that the robot either achieves a comparable pose or can achieve a comparable pose, and vice versa.

Estimating $RSSI$ for a given antenna pose, P, would require that the robot physically move the antenna to the pose and collect multiple samples from $RSSI$. Finding the

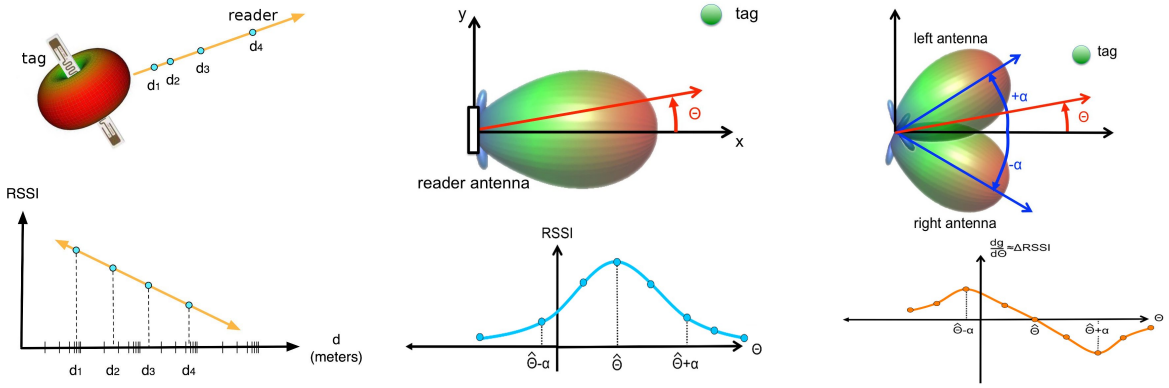

Fig. 3. **Left:** With constant orientation between the tag and reader antennas (top), RSSI strictly decreases with increasing distance, d. **Middle:** With constant positions for the tag and reader antennas and a fixed tag orientation (top), rotating the reader antenna about its z-axis yields a function of RSSI vs. Θ with a maximum when it is pointing at the tag (bottom). **Right:** Two reader antennas offset from one another by $2 * \alpha^{\circ}$ (top). The difference in their RSSI readings as they are rotated together (bottom) approximates the gradient of the RSSI captured from a single rotating antenna (middle bottom).

true optimum, P^*, via brute-force in this matter is clearly unrealistic and would be impractical even if $RSSI$ were deterministic as a function of P. In order to efficiently find good poses with respect to this optimization problem, we have developed three robot behaviors that work together to find approximate solutions, $\hat{P}$.

A. Insights from the Radar Equation

UHF RFID tags harvest all of their operating power from nearby, interrogating readers. Following the RF energy from reader-to-tag and back provides insight into both tag detection and RSSI measurements.

The radar equation is a simplified line-of-sight model that is commonly used to estimate received signal strength in radar systems [23]. It makes no attempt to model non-ideal environmental conditions such as multipath, shadowing, diffraction, material properties, or atmospheric conditions, and thus it is an optimistic approximation to real-world performance. However, as in the radar literature, we use insights gleaned from the radar equation to describe the relevant relationships between the RFID reader antenna, the tag antenna, and expected RFID sensor measurements (tag detection and RSSI).

The radar equation predicts the power received by the reader, P_{rdr}^{inc}, as a function of the distance, d (in meters), between the tag antenna and the reader antenna and the antennas' directional characteristics (gains, G_{rdr} and G_{tag}),

$$P_{rdr}^{inc}\ [\text{Watts}] \ \propto\ G_{tag}^2 \cdot \left(\frac{1}{d}\right)^4 \cdot G_{rdr}^2, \tag{2}$$

The antenna gains are polar functions of the azimuth and elevation angles from the antenna to the tag and are determined by the physical characteristics of the antennas. Often the gains are non-isotropic, so the relative orientation (6-DoF) between the reader and tag antennas is relevant. For example, Figure 3 shows the radiation patterns in free space for the tag antennas and reader antennas that we used in our experiments.

In our experiments, we used a ThingMagic M5e UHF RFID reader unit. The manufacturer states that the measured RSSI has a linear relationship to the RF power received by the reader in logarithmic units, decibel Watts or dBW,[1]

$$RSSI \propto P_{rdr}^{inc}\ [\text{dBW}] = 10 \cdot \log\left(P_{rdr}^{inc}\ [\text{Watts}]\right). \tag{3}$$

An examination of the radar equation highlights the following two useful relationships:

RSSI vs. Distance: Consider a single ray emanating from the tag, as shown in Figure 3 (left). Given a fixed tag-to-reader antenna orientation, the antenna gain terms in the radar equation (Equation 2) will remain constant so that,

$$P_{rdr}^{inc}\ [\text{Watts}] \ \propto\ \left(\frac{1}{d}\right)^4, \text{ and} \tag{4}$$

$$RSSI \ \propto\ P_{rdr}^{inc}\ [\text{dBW}] \ \propto\ -\log(d). \tag{5}$$

In this scenario, RSSI strictly increases as the distance between the reader and tag antennas decreases.

RSSI vs. Bearing Angle: Consider an RFID reader antenna and tag antenna at a fixed pose relative to one another, as shown in Figure 3 (middle). If the reader antenna is rotated about a fixed axis (i.e. its z-axis), then both the distance d and the tag antenna gain G_{tag} remain constant so that the power received at the reader (and thus RSSI) will be proportional to a cross section of the reader antenna's radiation pattern, $G_{rdr}(\Theta)$,

$$P_{rdr}^{inc}\ [\text{Watts}] \ \propto\ G_{rdr}(\Theta), \text{ so that} \tag{6}$$

$$RSSI \ \propto\ P_{rdr}^{inc}\ [\text{dBW}] \ \propto\ G_{rdr}(\Theta)\ [\text{dB}] \tag{7}$$

when the antenna gain is expressed in dB, as commonly supplied by antenna manufacturers. By employing a directional antenna which is unimodal and has a unique maximum

[1]We treat the ThingMagic RFID reader as a black box. The actual RSSI measurement provided by the reader is unitless and not calibrated to any physical unit, such as Watts (dBW) or milli-Watts (dBm). It is also dependent on an advanced digital signal processing pipeline that performs filtering, equalization, and noise de-correlation.

for each cross-section, as in this work, the function of RSSI versus bearing angle, Θ, will also be unimodal with a unique maximum. This maximum occurs precisely when the reader antennas is pointed at the tag.

B. Optimization of the Antenna's 6-DoF Pose

Consider a tag in unobstructed free space and a robot that can move its reader antenna to all antenna poses, P, by changing the antenna's Cartesian location, $< X, Y, Z >$, and orientation, $< \Theta, \Phi >$. At each location, the "RSSI vs. Bearing" relationship predicts a maximum RSSI when the antenna is directly pointed at the tag. The second relationship, "RSSI vs. Distance," predicts that RSSI strictly increases as the distance between the antenna and tag decreases, up until a maximum value when the antenna is as close as possible to the tag. Since there are no obstructions, the robot can follow a straight line toward the tag from any location until it reaches a maximum, at which point it will be pointed at the tag and adjacent to it. Any location that is not adjacent to the tag will not result in a maximal RSSI reading, so the optimal poses for our optimization problem must be pointed at the tag and adjacent to it.

Under practical conditions, the presence of obstacles combined with non-isotropic antenna radiation patterns may cause non-optimal final robot poses using this algorithm – a topic we will touch upon again in Section VI-A.

IV. Optimization Behavior for Global Search

The time requirements to perform exhaustive 6-DoF sampling of an indoor environment, such as a home, would be prohibitive. Instead, we use sparse sampling constrained to a plane, reducing the search to occur over Cartesian position and orientation of an antenna, <X,Y,Θ>. This is an approximation, since tags above or below the reader antenna plane can negatively impact performance. Our RFID search optimization becomes

$$< X^*, Y^*, \Theta^* >= \underset{x,y,\theta}{\operatorname{argmax}} \ \mathsf{E}(\ \boldsymbol{RSSI} \mid \boldsymbol{X} = x, \boldsymbol{Y} = y, \boldsymbol{\Theta} = \theta\ ). \quad (8)$$

Furthermore, we do not exhaustively sample pose, but rather perform sparse sampling at a specified spatial resolution. This yields a final pose in the local basin of attraction, which other robot behaviors seek to improve upon. Our global RFID search behavior occurs in two distinct phases:
(1) Sparse Sampling: The robot moves its reader antenna to many different poses across the entire environment and at each pose queries for *all tags*. For each positive tag detection, the robot records its pose on a map, the reader antenna's pose on a map, the tag's ID, and the RSSI measurement.
(2) Return to Pose with Maximum RSSI: Given a target tag ID, the robot uses the previously-captured data to solve the optimization in Equation 8: The robot identifies the antenna pose that yielded the maximum expected RSSI measurement for the target tag. The robot navigates back to the corresponding robot pose, and it orients its reader antenna to point in the direction corresponding to the maximal reading.

Fig. 4. The PR2 was commanded to perform sparse global RFID search with a 1.5 m resolution, constrained by the red rectangular search region. An overhead map of the home shows the robot-generated navigation waypoints (blue arrows), the robot's actual search path (blue line), tag positions (green circles), and navigation obstacles (purple regions).

A. Implementation

We used two articulated Laird Technologies S9025P UHF patch antennas (5.5 dB gain and 100° 3 dB beamwidths) and a ThingMagic M5e UHF RFID reader unit (1 Watt RF output power) affixed to a PR2, as shown in Figure 2. Under these conditions, the robot was able to detect UHF RFID tags up to 3 m under practical conditions, or exceeding 6 m under ideal line-of-sight conditions. The system provided 8-bit RSSI for each tag detection and could perform RFID measurements at 12 Hz, yielding up to 150 tag reads per second (query-mode) or 12 reads per second for a specific tag ID.

To perform sparse sampling the PR2 held its antennas at a fixed height, with the antennas' main beams parallel to the ground. The PR2 panned its left and right patch antennas back-and-forth at 30 °/s while querying for all tags in the environment, performing measurements evenly between the left and right antennas. At the same time, the PR2 navigated between a series of robot-generated waypoints. It programatically generated the waypoints based on a hand-specified rectangular search area and search resolution, as shown in Figure 4. The PR2 used SLAM to determine its pose on a previously-captured map of the environment, and used a Dynamic Window Approach (DWA) planner to move between waypoints. While moving, it constantly monitored for collisions and obstacles using planar and tilting laser rangefinders [24]. It discarded individual waypoints if the DWA's local path planner deemed them unreachable. We selected a search resolution of 1.5 m. At this resolution, sparse sampling required approximately 3 minutes to search the 9 m by 5 m area. At this rate, we estimate that the PR2 could sample the entire floor plan of an average American home (225 m^2 [25]) in fewer than 15 min, potentially at night, periodically in the day, or on demand.

After sparsely sampling the environment, the PR2 stopped and waited. Once tasked with locating a particular tag ID, it returned to the pose with maximum RSSI for the target tag. Due to sparse sampling of RSSI vs antenna pose, computing a sample mean was impractical. We instead used the raw maximum value, which worked well in practice.

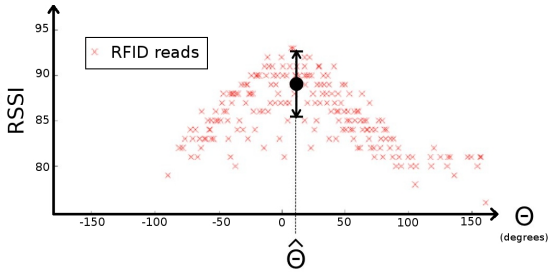

Fig. 5. This data was recorded from a reader antenna mounted to the head of a PR2 robot while the robot's head rotated. Actual RSSI measurements as a function of θ are noisy, so we model them as samples from a random variable, $\boldsymbol{RSSI}$, and optimize for expected value. For this particular scenario $\hat{\Theta} = 10^\circ$ and the true bearing $\Theta = 6^\circ$ (details in [27]).

V. Optimization Behaviors for Local Search

A. A Bearing Estimation Behavior

A straight-forward implementation of the "RSSI vs. Bearing Angle" relationship from Section III-A is to have a robot mechanically pan its reader antenna while capturing RSSI measurements. In the context of our general optimization framework (Equation 1), bearing estimation corresponds to the following simplification,

$$\hat{\Theta} = \underset{\theta}{\operatorname{argmax}} \ \mathsf{E}(\ \boldsymbol{RSSI} \mid \boldsymbol{\theta} = \theta\ ). \tag{9}$$

The angle that yields the maximum mean RSSI nominally corresponds to the bearing toward the tag, as shown in Figure 5. This approach is similar to early azimuth-only target acquisition radars that were used to locate and track aircraft [23], and can be extended to both azimuth and elevation bearing estimation [26]. In a large uncluttered room, we demonstrated that bearing estimation was capable of providing estimates accurate to within 20° when the robot was relatively close to the tag. However, estimation accuracy fell off as the maximum RSSI decreased (to less than 60° accuracy near the limits of the tag's read range)(details in [27]). Bearing estimation might be improved by taking more samples, by employing antennas with a narrower beamwidth, or by performing functional fits to the measured data.

B. A Servoing Behavior that Approaches Tagged Objects

By pointing two unimodal, smoothly varying patch antennas in different directions, we can efficiently estimate the gradient of RSSI with respect to rotation in Θ. Specifically, we use antennas at fixed offset angles, $\pm\alpha^o$, to compute a first-order central difference approximation of the gradient. We then rotate the robot, and hence the two antennas, at an angular velocity, $\dot{\Theta}$, proportional to this estimated gradient, and thereby locally maximize RSSI with respect to Θ.

$$\dot{\Theta} \propto \left.\frac{dg}{d\theta}\right|_{\Theta} \approx \frac{G_{rdr}(\Theta+\alpha) - G_{rdr}(\Theta-\alpha)}{2\alpha}, \tag{10}$$

where $G_{rdr}(\Theta+\alpha)$ is proportional to the RSSI of the left antenna ($RSSI_L$) and $G_{rdr}(\Theta-\alpha)$ is proportional to the RSSI of the right antenna ($RSSI_R$). Substituting this approximation into a feedback controller, we define bearing-only RFID servoing as:

$$\Delta RSSI = RSSI_L - RSSI_R \tag{11}$$

$$\dot{\Theta} = \kappa \cdot \Delta RSSI. \tag{12}$$

where κ is the controller's manually-tuned proportional gain. Intuitively, the difference between the left and right RSSI, $\Delta RSSI$, gives an indication of which direction the robot should turn so as to face the tag. If the left antenna receives a stronger RSSI, the robot should turn left. If the right antenna receives a stronger RSSI, the robot should turn right.

We model the left and right RSSI measurements as independent random variables ($\boldsymbol{RSSI_L}$ and $\boldsymbol{RSSI_R}$) and alter the robot's angular velocity in proportion to the expectation of the random variable, $\boldsymbol{\Delta RSSI} = \boldsymbol{RSSI_L} - \boldsymbol{RSSI_R}$ by

$$\begin{aligned}\mathsf{E}(\ \boldsymbol{\Delta RSSI} \mid \boldsymbol{\theta} = \theta\ ) = \quad & \mathsf{E}(\ \boldsymbol{RSSI_L} \mid \boldsymbol{\theta} = \theta\ ) \\ - \quad & \mathsf{E}(\ \boldsymbol{RSSI_R} \mid \boldsymbol{\theta} = \theta\ )\end{aligned} \tag{13}$$

$$\dot{\Theta} = \kappa \cdot \mathsf{E}(\ \boldsymbol{\Delta RSSI} \mid \boldsymbol{\theta} = \theta\ ). \tag{14}$$

Rotating the entire robot results in bearing-only RFID servoing with a feedback controller that adjusts the robot's heading so the robot orients toward the tag. Unlike bearing estimation, which required that the tag remain at a fixed position while articulating the reader antenna, bearing-only RFID servoing continuously updates the robot's heading even as a tagged object moves. This enables the robot to approach a tag by moving forward at a constant velocity while continuously updating its angular velocity and halting when its forward path is impeded by an obstacle, as detected by laser range finders. In practice, the forward velocity and κ must to be tuned to achieve good performance. For example, the forward velocity needs to be low enough to allow the robot to orient to the tag, but fast enough to make the behavior efficient.

1) Experiment and Evaluation: Our bearing-only RFID servoing system is analogous to conical scan radars. The radar literature refers to α as a *squint angle* and suggests using values that are 28-45% of the antennas' 3 dB beamwidth [28]. For our system, we selected $\alpha = 40^o$, which is 40% of the antennas' 3 dB beamwidths. As shown in Figure 2, our antennas are not located at the same origin due to physical constraints and robot mounting considerations. Instead, we mounted them on the robot's shoulders. We employ a five point moving average filter to estimate the expected value of RSSI for the left and right antennas. The ThingMagic reader returns RSSI values between 72 and 105, inclusive. We assign an RSSI value of 69 when a tag is not detected, since a lack of detection is associated with low received signal strength. Thus, $|\Delta RSSI| \in [0, 36]$. Hand-tuning for responsiveness, we selected a constant forward velocity of $10\,\mathrm{cm/s}$ and manually tuned the proportionality constant $\kappa = 1.15\,^\circ/\mathrm{s}$ to yield angular velocities $|\dot{\Theta}| \in [0, 41.4]\ ^\circ/\mathrm{s}$.

We also evaluated RFID servoing in a large uncluttered room. When the PR2 was within 3 m of the tag and initially

Fig. 6. **Top Left:** The Georgia Tech Aware Home where we tested our approach. **Top Right:** The nine tagged objects we used to evaluate our approach. From left-to-right: cordless phone, hair brush, TV remote, medication box, keys, medication bottle, water bottle, vitamin bottle, and teddy bear (toy). We tagged objects with Alien ALN-9640 Squiggle tags, with the exception of the TV remote and keys, which we tagged with Sontec metal-mount tags. **Bottom:** Photographs of the nine different test locations in the Aware Home's kitchen, dining, and living rooms.

oriented within $\pm 90^\circ$ of the ground-truth heading (i.e. well-matched to the final conditions provided by sparse global search followed by bearing estimation), the PR2 successfully approached the tag in 43/44 (97.2%) trials (details in [27]).

VI. Finding and Navigating to Tagged Objects in the Home

Input: Search resolution of $1.5\,\mathrm{m}$
Input: Bounding rectangle for search region
for $i = 1$ *to* 9 **do**
  Researcher: Place one tagged object in each location;
  Robot: Perform "Initial Sparse Sampling" phase of global search;
  foreach *Tagged Object ID* **do**
    Researcher: Command robot to find the tagged object;
    if *Not found during sparse sampling* **then**
      Robot: Break. Record "Tag not found";
    end
    Robot: Perform "Return to Pose" phase of global search;
    Robot: Perform Bearing Estimation;
    Robot: Perform RFID Servoing;
    Robot: Break. Record robot pose as result;
  end
  Researcher: Relocate objects to new locations;
end

Fig. 7. The experimental procedure we used to evaluate our system at the Georgia Tech Aware Home.

By combining the sparse global search behavior with the two local optimization behaviors, we enabled a mobile robot to find and navigate to tagged objects in a home. The robot first performed the global search behavior to find an initial robot configuration within the neighborhood of each tagged object it detected. It then moved to this configuration for a selected tag, used bearing estimation to point toward the tag, and used RFID servoing to approach the tag until impeded by an obstacle. Combined, these three behaviors result in a method that is straightforward to implement, does not require extensive data-driven training or calibration to build sensor models, and results in robot configurations that are both close to the desired tagged object and oriented toward it.

We evaluated our system in the Georgia Tech Aware Home, a realistic home environment shown in Figure 6, using nine tagged objects and nine different locations within the home. The PR2 autonomously performed the sampling phase of global RFID search nine times. Prior to each sampling, we placed one tagged object in each location. This resulted in 81 total object searches with each object in each location. Figure 7 summarizes the experimental process.

During the sampling phases, the robot obtained positive tag detections for the tagged objects in 69 out of 81 trials. In 12 instances the desired tagged object went undetected, resulting in "tag not found" failures. The failures occurred for the TV remote (7 failures), the keys (4 failures), and the hair brush on the floor (1 failure). The failures for the TV remote and keys are likely attributable to the heavy presence of metallic components interfering with RF signals. Despite using on-metal tags, these objects were not detected. Designing tag antennas for use on metal, near liquids, and affixed to people is an ongoing area of research. Additionally, we chose a $1.5\,\mathrm{m}$ search resolution for our experiments;

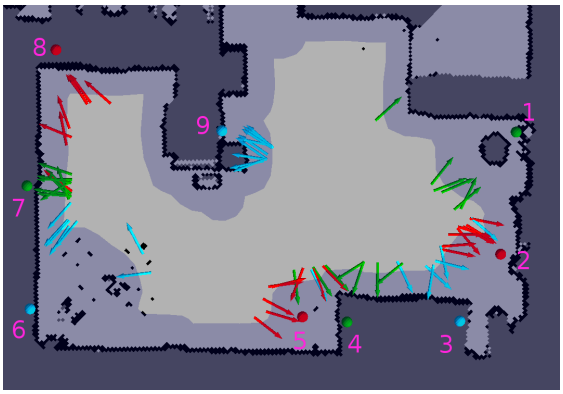

Fig. 8. The colored spheres on this map represent the locations of the tagged objects. Each colored arrow shows the robot's final pose after finding and navigating to the object with the same color.

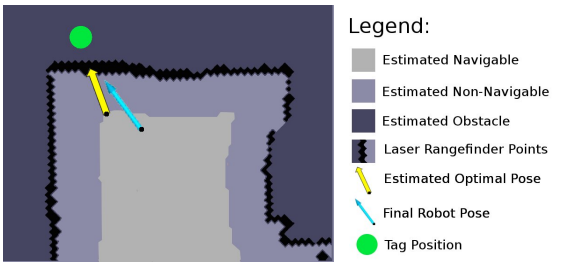

	Estimated Optimal	Final Robot Pose
Distance From Tag:	$d_{best} = 0.83\,\mathrm{m}$	$d_{final} = 1.14\,\mathrm{m}$
Robot's Heading:	$-30.2°$	$\theta_{heading} = -46.6°$
Bearing Toward Tag:	$-30.2°$	$\theta_{bearing} = -44.2°$

$$d_{err} = |d_{final} - d_{best}| = 0.31\,\mathrm{m}$$
$$\theta_{err} = |\theta_{heading} - \theta_{bearing}| = 2.4°$$

Fig. 9. The PR2 is incapable of navigating to all positions in the Georgia Tech Aware Home due to obstacles. The diagram and calculations above illustrate an example error calculation for one instance of RFID search for a specific tagged object (green dot). The yellow arrow shows the estimated optimal pose, which is the navigable location that is closest to the tagged object and oriented directly toward it. The blue arrow shows the final pose of the robot after actually finding and navigating to the target object using our three RFID search behaviors. The figure also shows d_{err} and θ_{err} for this navigation attempt. These specific results correspond with Figure 1.

searching with a finer resolution might have resulted in positive tag detections.

In the remaining 69 trials with at least one positive tag detection, the PR2 returned to the position and orientation with the maximum RSSI as part of the second phase of global search (Section IV). The PR2 then performed the two local optimization-based behaviors: bearing estimation (Section V-A) and RFID servoing (Section V-B). Figure 10 shows photographs of the final robot positions for several trials. Figure 8 shows the final poses of the robot obtained for all 69 trials. The supplementary materials include a video of the PR2 finding and navigating to a medication box inside a kitchen cabinet with a wooden door.

A. *Quantifying Performance*

Because of the arrangement of furniture and other obstacles, the best distance, d_{best}, achievable for each test location varied and depended on the robot's shape and navigation capabilities. We measure navigation error in terms of a distance error, d_{err}, and an angular error, θ_{err}. d_{err} compares the robot's final distance from the target object, d_{final}, with the estimated best achievable distance, d_{best}, using $d_{err} = |d_{final} - d_{best}|$. θ_{err} compares the robot's final heading, $\theta_{heading}$, with the target tag's actual bearing from the robot's final position, $\theta_{bearing}$, using $\theta_{err} = |\theta_{heading} - \theta_{bearing}|$. A sample calculation is shown in Figure 9.

We used the robot and its navigation system to estimate the navigable positions within the Georgia Tech Aware Home, which Figure 8 shows in light gray. For example, in location #2 (the fireplace mantle in Figure 6) the robot is at best capable of being within $0.54\,\mathrm{m}$ (planar distance) of the tagged object using this navigation system. In location #6, where the object is blocked by the kitchen table, the robot is at best capable of being within $1.53\,\mathrm{m}$ of the tagged object. In order to calculate d_{err} for the final pose achieved by the robot, we estimated d_{best} as the distance between the target object and the location closest to the target object that the robot had previously estimated as being navigable. We assumed that the robot could always orient itself so that $\theta_{err} = 0°$. Figure 9 also illustrates this calculation.

Across the 69 positive trials, the average distance error was $d_{err} = 0.36\,\mathrm{m}$ with standard deviation $\sigma = 0.33\,\mathrm{m}$, and the average angular error was $\theta_{err} = 23.2°$ with standard deviation $\sigma = 19.0°$.

The robot's estimates of the achievable locations play a role in our error measures. For one of the 9 test locations, these estimates were in error, since the robot navigated through locations that were estimated to be unachievable (see Figure 8, location #9). Our choice of error measure, $d_{err} = |d_{final} - d_{best}|$, penalizes final poses that actually get closer than the pose estimated as the closest achievable.

VII. Conclusion

UHF RFID tags could help address some of the challenges that robots face in unstructured environments and hasten the deployment of useful robots in homes and other environments. We presented our approach to finding and navigating to UHF RFID tagged objects, which does not require an explicit sensor model and performs well in practice. We formulated finding and navigating to an object as an optimization problem where the robot must find a pose of a directional antenna that maximizes the signal strength (RSSI) received from the target tag. We also developed and tested robot behaviors for global search, bearing estimation, and RFID servoing. We provided justification for our overall approach and these three behaviors using an idealized model of signal propagation from the radar literature. In our main experiment, we demonstrated that our behavior-based RFID search methods can be combined to find and navigate to UHF RFID tagged household objects in a realistic home environment without relying on training data or explicit sensor models.

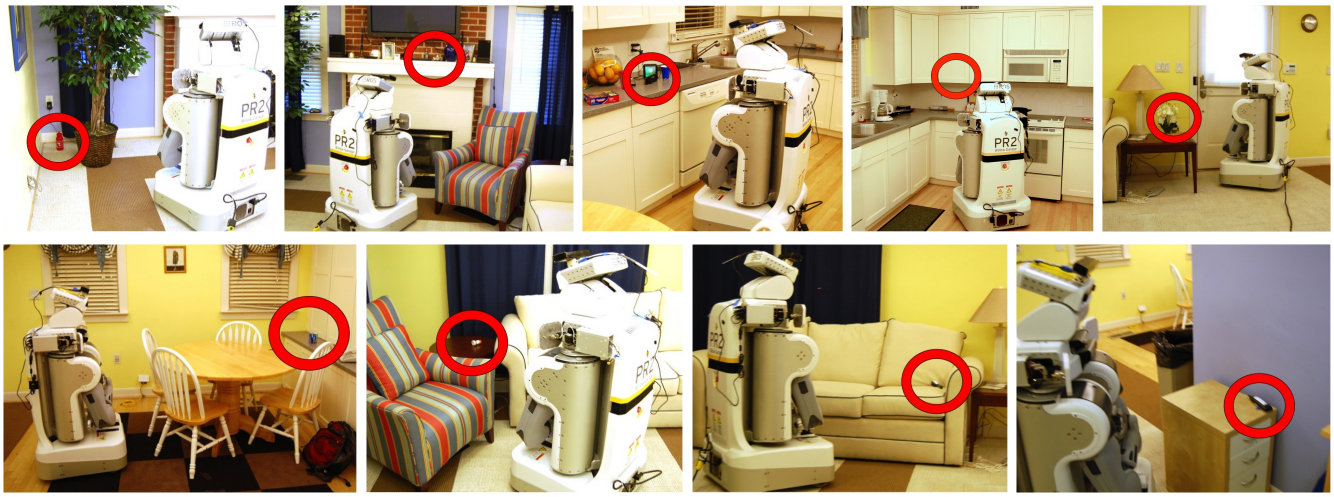

Fig. 10. Final robot configurations after finding and navigating to an object at each of the nine object locations in the Georgia Tech Aware Home.

Acknowledgments: *This work was supported in part by NSF grants CBET-0932592 and CBET-0931924, an NSF GRFP, and the Willow Garage PR2 Beta Program.*

REFERENCES

[1] EPC Global US, "Class 1 Generation 2 UHF RFID protocol for operation at 860MHz-960MHz, version 1.0.9," Available online, *http://www.epcglobalus.org/*.

[2] E. Schuster, S. Allen, and D. Brock, *Global RFID: the value of the EPCglobal network for supply chain management*. Springer Verlag, 2007.

[3] R. Rusu, B. Gerkey, and M. Beetz, "Robots in the kitchen: Exploiting ubiquitous sensing and actuation," *Robotics and Autonomous Systems*, vol. 56, no. 10, pp. 844–856, 2008.

[4] A. Kleiner, J. Prediger, and B. Nebel, "RFID technology-based exploration and SLAM for search and rescue," in *Proc. of the IEEE/RSJ International Conference on Intelligent Robots and Systems (IROS)*, 2006, pp. 4054–4059.

[5] J. Bohn and F. Mattern, "Super-distributed RFID Tag Infrastructures," *Lecture Notes in Computer Science*, pp. 1–12, 2004.

[6] B. Choi and J. Lee, "Mobile robot localization in indoor environment using RFID and sonar fusion system," in *IEEE/RSJ International Conference on Intelligent Robots and Systems (IROS)*, 2009, pp. 2039–2044.

[7] T. Deyle, C. C. Kemp, and M. S. Reynolds, "Probabilistic UHF RFID tag pose estimation with multiple antennas and a multipath RF propagation model," *IEEE/RSJ International Conference on Intelligent Robots and Systems (IROS 2008).*, pp. 1379–1384, 2008.

[8] S. Schneegans, P. Vorst, and A. Zell, "Using RFID Snapshots for Mobile Robot Self-Localization," in *Proceedings of the 3rd European Conference on Mobile Robots (ECMR 2007)*, 2007, pp. 241–246.

[9] D. Hahnel, W. Burgard, D. Fox, K. Fishkin, and M. Philipose, "Mapping and localization with RFID technology," in *Proceedings of IEEE International Conference on Robotics and Automation (ICRA)*, vol. 1, 26 April-1 May 2004, pp. 1015–1020.

[10] D. Joho, C. Plagemann, and W. Burgard, "Modeling RFID signal strength and tag detection for localization and mapping," in *Proceedings IEEE International Conference on Robotics and Automation (ICRA), Kobe, Japan.*, 2009, pp. 3160–3165.

[11] K. Finkenzeller and D. Müller, *RFID Handbook: Fundamentals and Applications in Contactless Smart Cards, Radio Frequency Identification and Near-Field Communication*. Wiley, 2010.

[12] A. Rahmati, L. Zhong, M. Hiltunen, and R. Jana, "Reliability techniques for RFID-based object tracking applications," in *IEEE/IFIP International Conference on Dependable Systems and Networks, 2007. (DSN 2007).* IEEE, 2007, pp. 113–118.

[13] A. Lázaro, D. Girbau, and D. Salinas, "Radio link budgets for UHF RFID on multipath environments," *IEEE Transactions on Antennas and Propagation.*, vol. 57, no. 4, pp. 1241–1251, 2009.

[14] D. Zarzhitsky, D. Spears, and W. Spears, "Distributed robotics approach to chemical plume tracing," in *IEEE/RSJ International Conference on Intelligent Robots and Systems (IROS 2005)*, 2005, pp. 4034–4039.

[15] R. Arkin, *Behavior-based robotics*. The MIT Press, 1998.

[16] R. Russell, A. Bab-Hadiashar, R. Shepherd, and G. Wallace, "A comparison of reactive robot chemotaxis algorithms," *Robotics and Autonomous Systems*, vol. 45, no. 2, pp. 83–97, 2003.

[17] J. Li, Q. Meng, Y. Wang, and M. Zeng, "Odor source localization using a mobile robot in outdoor airflow environments with a particle filter algorithm," *Autonomous Robots*, vol. 30, no. 3, pp. 281–292, 2011.

[18] D. Arnitz, "Tag localization in passive UHF RFID," PhD thesis, Graz Univ. of Techn., Austria, 2011. [Online]. Available: http://www.spsc.tugraz.at/publications

[19] A. Milella, D. Di Paola, G. Cicirelli, and T. D'Orazio, "RFID tag bearing estimation for mobile robot localization," in *International Conference on Advanced Robotics, 2009. ICAR 2009.* IEEE, 2009, pp. 1–6.

[20] M. Kim, N. Chong, and W. Yu, "Robust DOA estimation and target docking for mobile robots," *Intelligent Service Robotics*, vol. 2, no. 1, pp. 41–51, 2009.

[21] R. Liu, P. Vorst, A. Koch, and A. Zell, "Path following for indoor robots with RFID received signal strength," in *IEEE International Conference on Software, Telecommunications and Computer Networks (SoftCOM)*, 2011, pp. 1–7.

[22] T. Deyle, H. Nguyen, M. Reynolds, and C. Kemp, "RFID-guided robots for pervasive automation," *IEEE Pervasive Computing*, vol. 9, pp. 37–45, 2010.

[23] M. Skolnik, *Introduction to Radar Systems*. McGraw-Hill New York, New York, USA, 1962.

[24] E. Marder-Eppstein, E. Berger, T. Foote, B. Gerkey, and K. Konolige, "The office marathon: Robust navigation in an indoor office environment," in *Proceedings of IEEE International Conference on Robotics and Automation (ICRA 2010).* IEEE, 2010, pp. 300–307.

[25] (2013, June) Median and average square feet of floor area in new single-family houses completed by location. [Online]. Available: http://www.census.gov/const/C25Ann/sftotalmedavgsqft.pdf

[26] T. Deyle, H. Nguyen, M. Reynolds, and C. C. Kemp, "RF Vision: RFID Receive Signal Strength Indicator (RSSI) Images for Sensor Fusion and Mobile Manipulation," *IEEE/RSJ International Conference on Intelligent Robots and Systems (IROS 2009).*

[27] T. Deyle, "Ultra High Frequency (UHF) Radio-Frequency Identification (RFID) for Robot Perception and Mobile Manipulation," Ph.D. dissertation, Georgia Institute of Technology, 2011.

[28] G. Brooker, "Conical-scan antennas for W-band radar systems," in *Proceedings of the International Radar Conference.* IEEE, 2003, pp. 406–411.